

HIGHER SCHOOL OF ECONOMICS  
NATIONAL RESEARCH UNIVERSITY

**CONSTRUCTING AN EFFICIENT  
MACHINE LEARNING MODEL  
FOR TORNADO PREDICTION**

Working Paper WP7/2016/05  
Series WP7

Mathematical methods  
for decision making in economics,  
business and politics

Moscow  
2016

УДК 504.056  
ББК 20.1  
С75

Editors of the Series WP7  
“Mathematical methods for decision making  
in economics, business and politics”  
*Aleskerov Fuad, Mirkin Boris, Podinovskiy Vladislav*

C75 **Constructing an efficient machine learning model for tornado prediction** [Text] : Working paper WP7/2016/05 / F. Aleskerov, N. Baiborodov, S. Demin, S. Shvydun, T. Trafalis, M. Richman, V. Yakuba ; National Research University Higher School of Economics. – Moscow : Higher School of Economics Publ. House, 2016. – 24 p. – (Series WP7 “Mathematical methods for decision making in economics, business and politics”). – 35 copies.

Tornado prediction methods and main mechanisms of tornado genesis were analyzed. A model, based on the superposition principle, has been built. For efficiency evaluation, the constructed model has been tested on real-life data obtained from the University of Oklahoma (USA).

It is shown that the constructed tornado prediction model is more efficient than all previous models.

Key words: tornado prediction; superposition principle; data analysis

УДК 504.056  
ББК 20.1

*Fuad Aleskerov* – National Research University Higher School of Economics, V.A. Trapeznikov Institute of Control Sciences of Russian Academy of Sciences, Moscow, Russia.

*Nikita Baiborodov* – Moscow Institute of Physics and Technology, Moscow, Russia.

*Sergey Demin* – National Research University Higher School of Economics, Moscow, Russia.

*Sergey Shvydun* – National Research University Higher School of Economics, V.A. Trapeznikov Institute of Control Sciences of Russian Academy of Sciences, Moscow, Russia.

*Theodore Trafalis* – University of Oklahoma, USA.

*Michael Richman* – University of Oklahoma, USA.

*Vyacheslav Yakuba* – National Research University Higher School of Economics, V.A. Trapeznikov Institute of Control Sciences of Russian Academy of Sciences, Moscow, Russia.

© Fuad Aleskerov, 2016  
© Nikita Baiborodov, 2016  
© Sergey Demin, 2016  
© Sergey Shvydun, 2016  
© Theodore Trafalis, 2016  
© Michael Richman, 2016  
© Vyacheslav Yakuba, 2016  
© National Research University  
Higher School of Economics, 2016

# 1. Introduction

Tornadoes are a major disaster hazard. For instance, direct losses to the US economy, caused by tornadoes for the period from 2010 to 2014 were about 16.5 billion dollars (NOAA, US National Weather Service). Therefore, accurately forecasting these events as far in advance as possible is an important research activity.

However, achieving forecasts with long lead times is difficult because tornado genesis process is still not understood fully [Rasmussen et al., 2004]. Furthermore, it has been noted that a crucial part of the process is chaotic, which makes prediction of tornado even more complicated [Rhodes, Senkbeil, 2014].

The approach to model tornadogenesis using dynamic processes is time and resource consuming, and owing to the small scale of a tornado, physically-based numerical weather prediction models still do not provide very good results.

In this work we propose a new approach into disaster prediction by using the methods of intelligent data analysis for detecting tornadic circulations from the set of all observations  $A$ . As a result, constructed models predict tornado occurrence with higher efficiency. In addition, intelligent data analysis methods work faster than simulation by dynamic weather prediction models, allowing extra time for reacting and preventing dangerous repercussions of the disaster.

The basic goal here is to find the main patterns between different characteristics of air circulation and, given these patterns, detect tornadoes. For this purpose, the following parameters of air circulations are used – temperature, air pressure, relative humidity, velocity of the air flow and many other physical characteristics of the near-storm atmosphere.

There are numerous procedures that allow choosing alternatives from the initial set. In this work, we consider choice procedures of a special type based on the superposition principle<sup>1</sup> [Aleskerov et al., 2014].

Superposition has several advantages. First, the computational complexity of the model can be managed. Unfortunately, most existing machine learning algorithms have a high computational complexity, so they cannot be applied in the case of large number of observations or/and criteria. The use of superposition allows reducing the complexity by applying methods with a low

---

<sup>1</sup> In some works the term “composition” is used instead of “superposition”.

computational complexity on first stages and more accurate methods on final stages. Consequently, our models can be applied to larger initial datasets.

Second, superposition allows us to combine different methods and use several criteria simultaneously on each step. Moreover, models based on the idea of superposition can be interpreted easily since we can apply several simple methods instead of a complicated one. In addition, superposition will help to reduce the influence of drawbacks of initial methods. Hence, our model may have advantages of all previous techniques.

## **Acknowledgement**

The article was prepared within the framework of the Basic Research Program at the National Research University Higher School of Economics (HSE) and supported within the framework of a subsidy by the Russian Academic Excellence Project “5–100”.

## **2. Literature review**

We consider here only the studies on application of intelligent data analysis methods to the tornado prediction.

Adrianto et al. [2009] proposed the use of support vector machines (SVM) for tornado prediction, i.e. the algorithm constructs a hyperplane that separates a set of elements into two classes (e.g., tornadoes and non-tornadoes).

The defining function is presented as a dot product of two vectors. The first one is a vector of circulation attributes, such as wind speed, temperature, air pressure on the surface, relative humidity at different levels, etc. In turn, the second vector consists of weight coefficients, which show the importance of each parameter in tornado prediction process. So, small absolute value of weight coefficient means that the parameter almost cannot influence future tornado detection. Correspondingly, high value of the coefficient indicates high prediction power of the attribute.

However, the accuracy of all methods based on linear regression is very low. Recently, Trafalis et al. [2014] also proposed other approaches to this problem.

The first mentioned technique is an improvement of the aforementioned method of support vector machines with reverse features elimination (SVM-

RFE). According to this approach, one should realize the standard SVM algorithm and get weight coefficients. Afterwards the attribute which has the lowest value of the weight coefficient is eliminated from the features list. Subsequently, the algorithm iteratively continues until only one parameter remains.

At the end of the process, the sequence of eliminated attributes transforms into the ranking of the parameters by the following rule. The number of the attribute in the ranking is equal to the number of iterations (backward), when the attribute was eliminated.

However, the ranking is not the only goal of this method. Some features of air circulation might not help, but even interfere with tornado detection (giving false signals). Therefore, the last step of the SVM-RFE algorithm is choosing the number of parameters which are used for tornado detection. For this purpose, one evaluates the accuracy of the method according to the number of used attributes (it is important to point out that the algorithm uses only top attributes from the ranking).

One more method proposed for tornado prediction is a neural network approach [Marzban et al., 1996, Marzban, 2000, Lakshmanan et al., 2005]. The main idea is the construction of a non-linear function that maps real-valued input variables to a number varying from 0 to 1. The most popular version of neural network is used – three-layer perceptron network. Such a neural network has one hidden layer of neurons.

The next proposed technique is Random Forest method (RANF), developed by Breiman [2001]. It is a group classifier with multiple decision trees, wherein each tree is trained on a part of all attributes, chosen randomly. Consequently, the predictions of all trees are aggregated by the classification based on the majority of the votes over all classifiers.

The last proposed algorithm is Rotation Forest method (ROTF) by Rodriguez et al. [2006]. This method utilizes principal component analysis (PCA) to distinguish attributes which are used to construct a decision forest. This forest consists of decision trees which are trained on the whole data set in a rotated feature space. The set of parameters is randomly divided into K groups. Afterwards, principal component analysis is performed simultaneously on each group. As a result, we receive K classifiers that compose one classification instrument. This instrument works in the same way as RANF; classification is based on the majority of the votes over all of the trees.

It is important to point out that all the aforementioned methods have specific drawbacks, which decrease the accuracy of tornado prediction. Accord-

ing to the aforementioned previous studies, all techniques detect only a fraction of the tornadoes (more than 25% of all tornadoes are missed). In addition, a significant part of tornado signals (about 20%) is false alarm, which is also very important. Thus, general accuracy of these methods (from 51 to 57%) is not high enough for efficient application in real life, because such results slightly exceed tornado prediction by the coin toss.

In this work we use choice functions, based on the superposition principle [Aleskerov et al., 2014] to make tornado prediction. Usually a standard choice function  $C_1(\cdot)$  consists in the choice of some subset of alternatives that satisfy the predefined condition.

Ideally the specified condition should be “being tornadic circulation.” However, in real life it is difficult to satisfy this condition. Hence, we use some simpler conditions, which narrow the initial set of observations and get trustworthy results by application of the superposition principle.

Superposition of two choice functions  $C_1(\cdot)$  and  $C_2(\cdot)$  is a binary operation  $\odot$ , the result of which is a new function  $C^*(\cdot) = C_2(\cdot) \odot C_1(\cdot)$ , which has a form  $\forall X \in 2^A C^*(X) = C_2(C_1(X))$  [Aizerman, Aleskerov, 1995]. In short, the latter function  $C_2(\cdot)$  is used on the data obtained by the application of the former one  $C_1(\cdot)$ . It is necessary to mention that in the case of change of methods’ application order the result might be totally different, as the superposition is not commutative and the functions  $C_1(\cdot)$  and  $C_2(\cdot)$  can be completely diverse. The properties of the superposition operator were studied in [Aizerman, Aleskerov, 1995; Aleskerov, Cinar, 2008; Shvydun, 2015] and other papers.

### 3. Preliminary data analysis

#### 3.1. Data description

Here we use the same data as Trafalis et al. (2014). It is the dataset of meteorological parameters, circulations and observations calculated by application of the Mesocyclone Detection Algorithm (MDA) and near-storm environment (NSE) algorithm from Doppler radar velocity data. These two methods were developed at the National Severe Storms Laboratory [Kingfield et al., 2012]. The main idea of these methods is an analysis of azimuthal shear in Doppler radar velocity and rotational strength data in 3 dimensions.

In this dataset we have 10,816 observed circulations (721 of them are tornadic circulations) taken from 111 storm days. Unfortunately, these storm days are not consecutive – these circulations took place in the time period from 1995 to 1999. All observations contain 83 attributes, which describe physical characteristics like pressure, temperature, wind velocity, etc. In addition, one parameter shows the date of circulation occurrence (month). In turn, the target parameter is binary (tornado or non-tornado), which means that our problem is classification of these data into two classes.

Additionally, it is important to highlight some specific features of these data which interfere with tornado prediction. For instance, some observations account for one air circulation. The difference between them is explained by the fact that one mesocyclone was detected at different times by different radars.

Because, there is an assumption that the parameters leading to tornado-genesis are location invariant, a feature of the dataset is the absence of information about the place, where observation was made. Thus, we have neither information about any characteristics of observation location (hill existence or distance from the ocean, for instance), nor just approximate locality (for example, state).

### ***3.2. Data correction***

Any data mining process requires data preprocessing, such as deleting duplicate or outlying values and verification of value intervals. In addition, in some situations it can be important to check measure units.

Thus, we began examining the data in terms of outliers. For instance, attribute V23 (meso low-level convergence) for one circulation had a value equal to  $-32,768$ . In meteorological data sets, this undocumented value is normally taken as a flag for missing data. However, from the theoretical point of view the range of values for this parameter is from 0 to 70. Therefore, this observation was replaced by the mean value of the parameter.<sup>2</sup>

Afterwards we analyzed the data in terms of intervals of parameter values. Investigating all attributes one by one we got first hint for possible problems at V2 (meso base). The problem is that all values of the parameter lay from 0 to 229, although in theory they can reach the level of 12,000. Nevertheless, it

---

<sup>2</sup> At the next step we will use a better methodology to replace outliers, which is data imputation with machine learning algorithms [Richman et al., 2008].

is only a potential hint, because these data might be a real situation with a small range of the values takes place.

However, studying V4 (meso strength rank) we find one more hint for incorrect data. Namely, the values should be from 0 to 25, while in the dataset the range of the values is much wider – from 14 to 12,337. In addition, for V5 (meso low-level diameter) we can find a similar situation: theoretical range (0–15,000) and the real one (0–18) differ strongly from each other. Thereby we have the situation illustrated by Table 1. All discovered features allow us to propose the following hypothesis: parameters V3, V4, V5 should be shifted.

*Table 1.* Ranges of the attribute’s values

Attribute	V2	V3	V4	V5	V6	V7
Theoretical range	0–12,000	0–13,000	0–25	0–15,000	0–15,000	0–12,000
Real range	0–229	8–8,453	14–12,337	0–18	500–14,985	503–14,992

Thus, we may notice that the values of parameters V3, V4, V5, V6, V7 suit much better to the left neighbor attribute. The rest of the study is selecting the whole list of parameters, which need shift. For this purpose, we will continue to study ranges of the attribute values.

The last parameter is V25 (meso range), is suspicious, as the values of the next attribute (from 7,628 to 10,136) do not match; because the range of the mesocyclone equal to 8,000 km seems to be excessive. In turn, V2 values, which are not used now (they should be shifted to the V1, but that attribute has the right values), lie from 0 to 229. It means that these figures suit to V25.

So, the next data alteration is the following data shift: the values for V3 – V25 attributes are shifted to the previous attributes (for instance, V3 values are now V2 values). Meanwhile, V2 values go to V25.

At the next stage we noticed another specific data feature. V51 (magnitude of the low-level shear vector (surface to 3 km above ground level)) values are equal to the values of V66 (Average Relative Humidity in 0–1 km layer) for the majority of the circulations (5,171 of 5,409). Meanwhile, for the other 238 circulations V51 values are equal to the values of V67 (0–1 km shear magnitude).

Table 2. V51, V66-V74 attribute values

V51	V66	V67	V68	V69	V70	V71	V72	V73	V74
393	393	603	352	412	131	175	605	3446	153
314	314	597	300	361	127	139	661	3955	160
326	326	597	309	368	127	143	664	3806	161
320	320	599	305	367	125	142	670	3944	161
381	381	607	347	410	129	183	643	3496	163
441	441	594	372	431	144	197	481	3286	116
383	383	606	348	410	128	175	633	3482	161
331	331	597	313	371	128	145	661	3714	161
<b>384</b>	<b>86</b>	<b>384</b>	<b>607</b>	<b>348</b>	<b>411</b>	<b>133</b>	<b>193</b>	<b>643</b>	<b>3497</b>
394	394	604	352	414	134	186	610	3453	153
289	289	676	277	344	104	108	674	4892	123
325	325	597	309	368	127	143	665	3822	161
390	390	605	351	413	133	187	621	3467	156
416	416	601	361	423	142	207	560	3390	137

As an example, we present some values from the dataset (Table 2). In this example we have circulations with V51 equal to V66 and V67 (the latter is highlighted bold). It is important to point out that highlighted circulation has different values from all other data for attributes in the range V59–V76.

This data feature allows us to propose one more hypothesis; we need another shift in the dataset. However, we should decide what piece of data will be altered; either figures for 238 circulations or attribute values for 5,171 circulations. For this purpose, we study the attributes from the physical point of view.

The best parameter for this task is V66 (average relative humidity in 0–1 km layer). In the case of shifting 238 circulations’ figures, this attribute’s values will be up to 632, which is certainly extremely high value for this parameter. Because of it, we decided to shift the majority of circulations (V59–V76 will be shifted to the attribute with the higher number).

However, this data shift has crucial difference from the previous one. In the previous case V2 data went to V25. However, V77 values do not go to V59. The reason for this peculiarity is the fact that the range of V77 is equal to [–13,917; 20,170].

At the last stage of preliminary data analysis we study the values of the attributes in terms of the meaning of the circulation parameters. Here we are faced with some problems again. For instance, V26 (actual surface pressure) has values varying from 7,628 mb to 10,136 mb. Obviously, the decimal before the last digit is missing as taking into account the measure unit ( $1 \text{ mb} = 0.001 \text{ b} \approx 0.001 \text{ atm}$ ) that would be impossibly high pressure, up to 10 atmospheres. According to the same principle, we point out the list of parameters with “strange” range of the values. However, the decimal can be inserted and the problem will be eliminated.

### ***3.3. A correlation of the parameters***

When data preprocessing has been completed, we start data analysis. However, here we face another problem. Certainly, a large amount of data can give us a lot of information, which can help to predict a tornado. However, using of too much information may make our model excessively complicated. So, for the purpose of decreasing the amount of information analyzed, we have decided to examine the data more thoroughly and to choose parameters which will play greater role in our tornado prediction model.

For this purpose, we examined the correlation between different parameters to detect attributes with high correlation. These characteristics can be discarded, because we can predict the value of one parameter using the value of the other one. For instance, attributes V61 (Average Mixing Ratio in 0–1km layer) and V62 (Average Mixing Ratio in 0–3km layer) have correlation equal to 0,984. Taking into account this fact, we decided to use only one of these parameters.

Thus, in Table 3 we can see all pairs of attributes for which the absolute value of correlation coefficient is higher than 0,85. From each pair we discarded one of the attributes<sup>3</sup>. For this purpose, for each pair we studied which of the parameters belongs to a larger number of highly correlated pairs and rejected it.

It is important to mention that during parameter rejection we found not only pairs, but also triplets of attributes with high absolute value of correlation coefficient. For instance, one of such triplets consists of V2 (Meso base), V3 (Meso depth) and V18 (Meso core depth) and, according to the attribute correlation, we kept only one attribute from this triplet.

---

<sup>3</sup> Another option is forming a new composite variable by linear combination.

*Table 3.* Pairs of attributes with absolute value of correlation over than 0,85

<b>Attribute 1</b>	<b>Attribute 2</b>	<b>Correlation</b>
V61	V62	0,984
V46	V56	0,94
V3	V18	0,939
V2	V3	0,939
V35	V36	0,921
V67	V69	0,911
V34	V57	0,9
V2	V18	0,898
V69	V75	0,897
V51	V68	0,882
V11	V17	0,87
V4	V19	0,869
V40	V43	0,859
V31	V63	0,859
V37	V41	-0,862
V40	V41	-0,864
V50	V54	-0,874
V34	V58	-0,933
V57	V58	-0,935

### ***3.4. An analysis of the distribution of parameters***

The next step of choosing characteristics consists of choosing parameters which have different distribution of the tornadic and non-tornadic circulations. This procedure helps us to detect tornadoes in the following way. If a parameter has different distribution for circulations of different types, it has ranges, where tornadic circulations occur more rarely. As a result, we can be more confident that certain circulation is nontornadic.

For instance, on Figure 1 we can see the distribution of tornadic and non-tornadic circulations according to the parameter V3 (meso depth of the circu-

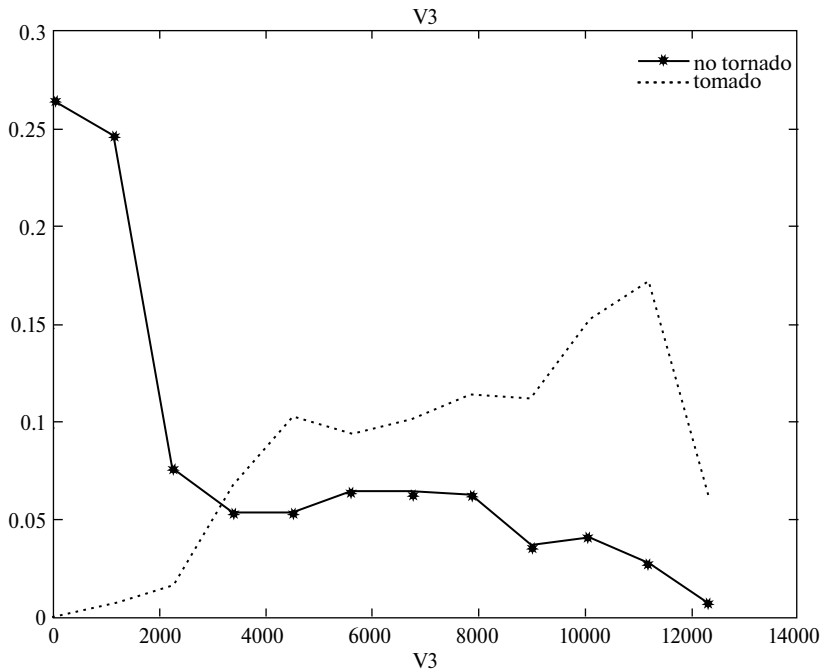


**Fig. 1.** Distribution of tornadic and non-tornadic circulation according to V3 (meso depth)

lation). For this parameter, if an element has a small value in the range 0–1,000 m, we can claim that it does not seem to be a tornado. Meanwhile, if the value is in the range 10,000–12,000 m, the circulation has higher possibility to become tornado.

### 3.5. Additional considerations

The next step will help us to add attributes of circulation, which have not been highlighted. These parameters can be important in tornado evolution process, so we studied the procedure of tornadic circulation formation paying attention to the physical processes.

At this stage we should remember that the main goal is prediction of tornados in advance, to have enough lead time to warn people. Therefore, only those selected parameters that aid in this goal should be used in our research.

To that end, we studied the tornadogenesis process from the physical point of view. As a result, we divided the list of all parameters into two parts: *a priori* characteristics, which give a signal for tornado occurrence beforehand, and *a posteriori* ones, which only fix the prediction when the disaster has already happened. For instance, such attribute as meso low-level rotational velocity might be good *a priori* predictor of tornadogenesis. However, in these data, we did not find evidence, that this is the case and excluded it. Afterwards choosing only *a priori* parameters gives us the final list of characteristics used in finding patterns.

## 4. Framework

Consider a finite set  $A$  of alternatives evaluated by  $n$  parameters, i.e. the vector of values  $(u_1(x), \dots, u_n(x))$  is assigned to each alternative  $x$  from  $A$ , i.e.,

$$x \in A \rightarrow (u_1(x), \dots, u_n(x))$$

The problem lies in constructing a transformation  $C(\cdot)$  – the rule of aggregation over  $A$  – such that  $C(\cdot): A \rightarrow R^1$ .

Our model is based on a superposition principle, applied for different choice functions. There are different ways on how to construct a choice function  $C(\cdot)$ . One of the options is provided below:

$$\forall X \subseteq AC(X) = \{y \in X | \alpha_i u_i(y) + \alpha_j u_j(y) \geq b\},$$

where  $u_i(\cdot)$  and  $u_j(\cdot)$  are the values of two exact parameters  $i, j \in \{1, \dots, n\}$  of an observation, while  $b$  is the threshold value that depends on the initial set  $X$  and chosen parameters  $i$  and  $j$ . In turn the values  $\alpha_i, \alpha_j$  are automatically defined by the following linear optimization problem

$$\left\{ \begin{array}{l} \min_{\alpha_i, \alpha_j} \sum_{l=1}^N e_l \\ e_l = \sqrt{(t_l - \hat{t}_l)^2} \forall l = 1, \dots, N \\ \hat{t}_l = \alpha_i u_i(y_l) + \alpha_j u_j(y_l) \forall l = 1, \dots, N, \end{array} \right.$$

where  $t_l$  is the variable, which shows the ground truth of  $l$ -th observation (tornado or no tornado);  $N$  – number of observations in the dataset  $X$ .

Note that other forms of the choice function can be used in the model.

As a result, we got a sequential pointing out group of tornadic observations (Fig. 2).



**Fig. 2.** Example of choice functions' superposition (inscriptions above the vertices present the parameters used at this stage)

The main idea of our model is the construction of a certain number of such superposition sequences in order to distinct tornadic and non-tornadic observations. Afterwards, we unite them and the resulting prediction of our model will be the union of observation sets, obtained by different superpositions.

## 5. Application of the model

As it was mentioned before, we apply our model to the preprocessed data obtained from the University of Oklahoma. For the correct application we need to construct training and testing datasets. According to the standard rules of data mining the whole dataset should be divided into two parts in the ratio 70:30, where the larger part is the training set.

However, here we face the following problem. At the end of the study we will compare our model with the previous ones. In their study Trafalis et al. [2014] used another separation ratio – they divided the original dataset into two equal parts. As a result, if we use the standard ratio, the comparison would not be correct, because increasing the size of training dataset improves the accuracy of the model. Thus, we decided to apply the model twice. The first application will use equal separation and help us to compare the results. In turn, the second application will use standard data division ratio and show the accuracy of the model in standard conditions.

After the data sampling, it is important to choose the metrics for model comparison/evaluation, because there are numerous available “efficiency calculations.” In Table 4 four of them are presented.

Table 4. Different efficiency calculation methods.

$tp$  – true positive prediction,  $fp$  – false positive prediction,  $tn$  – true negative prediction,  $fn$  – false negative prediction

Efficiency calculation method	Formula
Classification Accuracy	$CA = \frac{tp + tn}{tp + tn + fp + fn}$
Probability of Detection	$POD = \frac{tp}{tp + fn}$
False Alarm Ratio	$FAR = \frac{fp}{tp + fp}$
Critical Success Index	$CSI = \frac{tp}{tp + fp + fn}$

Analyzing the efficiency calculation methods, at the first stage we reject Probability of Detection and False Alarm Ratio, because any one of these techniques does not take into account significant part of the results. For instance, the former takes into consideration only predictions for tornadic circulations. In turn, the latter does not consider the number of missed tornadoes. Two methods would need to be examined to obtain a characterization of the model.

At the second stage we should choose between Classification Accuracy and Critical Success Index. Given the peculiarity of the data, wherein about 93% of observations are non-tornadic, we reject Classification Accuracy since if we use classification accuracy all models will have almost the same results. Thus, we choose Critical Success Index.

When all preparations are over we apply the constructed tornado prediction model and evaluate its efficiency. As a result, we obtained the following figures (Table 5) for 50:50 division ratio (the tornado prediction procedure was repeated 20 times and the value in Table 5.2 is the mean value).

In turn, in case of standard 70:30 data division for training and testing sets the efficiency of our model is even higher and equal to 0,63.

Comparing all tornado prediction methods in terms of three techniques of efficiency evaluation (POD, FAR and CSI), we will get the following Roebber's (2009) performance diagram (Fig. 3). As we can see, the improved de-

cision tree Pareto-dominates all other models except slight predominance of logistic regression in terms of probability of detection.

*Table 5.* Comparison of the constructed model with previous works.

Prediction technique	POD	FAR	CSI
SVM	0,68	0,22	0,57
Logistic regression	0,7	0,25	0,57
RANF	0,58	0,17	0,51
ROTF	0,61	0,21	0,53
Superposition with mixed parameters	0,68	0,16	0,61

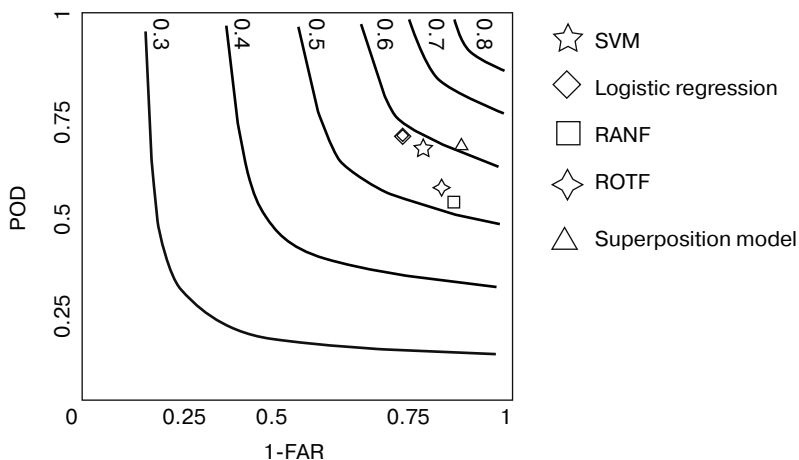


**Fig. 3.** Roebber's performance diagram for the performance results of all classifiers. The solid lines represent CSI

## 6. Conclusion

As expected, the results of improved decision tree model exceed the results of all models, which were applied before. The improvement arises as the false alarm ratio is notably smaller with this technique. There is a small trade-off of impressed misses, compared to logistic regression. According to mete-

orologists' opinion, a skill improvement equal to 0,05 is significant development. As CSI is an important component of skill, constructed model is a successful attempt to improve tornado prediction technique. Therefore, the improved decision tree model provides the best opportunity to provide accurate tornado formation predictions with sufficient lead times.

## Appendix 1 – list of attributes

Attribute number	Meaning of the attribute
V1	Month
V2	Meso base (m) [0–12000]
V3	Meso depth (m) [0–13000]
V4	Meso strength rank [0–25]
V5	Meso low-level diameter (m) [0–15000]
V6	Meso maximum diameter (m) [0–15000]
V7	Meso height of maximum diameter (m) [0–12000]
V8	Meso low-level rotational velocity (m/s) [0–65]
V9	Meso maximum rotational velocity (m/s) [0–65]
V10	Meso height of maximum rotational velocity (m) [0–12000]
V11	Meso low-level shear (m/s/km) [0–175]
V12	Meso maximum shear (m/s/km) [0–175]
V13	Meso height of maximum shear (m) [0–12000]
V14	Meso low-level gate-to-gate velocity difference (m/s) [0–130]
V15	Meso maximum gate-to-gate velocity difference (m/s) [0–130]
V16	Meso height of maximum gate-to-gate velocity difference (m) [0–12000]
V17	Meso core base (m) [0–12000]
V18	Meso core depth (m) [0–9000]
V19	Meso age (min) [0–200]
V20	Meso strength index (MSI) weighted by average density of integrated lyr [0–13000]
V21	Meso strength index (MSIr) “rank” [0–25]

Attribute number	Meaning of the attribute
V22	Meso relative depth (%) [0–100]
V23	Meso low-level convergence (m/s) [0–70]
V24	Meso mid-level convergence (m/s) [0–70]
V25	Meso Range (km) [0–230]
V26	Actual surface pressure (mb)
V27	Height of the 273 K temperature surface (m agl)
V28	Average wind speed over a specified depth (m/s)
V29	U – component of estimated storm motion vector (north–relative; m/s)
V30	V – component of estimated storm motion vector (north –relative; m/s)
V31	Estimated 0–3 km storm relative helicity ( $m^2/s^2$ )
V32	Surface relative humidity (percent)
V33	Surface virtual temperature (Kelvin)
V34	Downdraft CAPE (dCAPE) for a parcel 1 km AGL
V35	dCAPE for a parcel 3 km AGL
V36	dCAPE for the parcel at 0 Celsius
V37	Convective Available Potential Energy (CAPE) (J/kg) for a parcel with Average characteristics over the lowest X mb (e.g., 100 mb)
V38	Convective Available Potential Energy (CAPE) (J/kg) for Convective Inhibition (CIN)
V39	Same as 37, except for Level of Free Convection (LFC)
V40	Same as 37, except for Equilibrium Level (EL)
V41	Same as 37, except for Lifted Index (LI)
V42	Same as 37, except for Energy-Helicity Index (EHI)
V43	Average Parcel Level: level (m AGL) at which the negative area above the Surface-based CAPE counterbalances the surface–based CAPE.
V44	Magnitude of the storm–relative flow for the 0–2 km agl layer (kts). The estimated storm motion vector is subtracted from the average model wind vector of the layer.
V45	Same as 44, except for the 4–6 km agl layer
V46	Same as 44, except for the 9–11 km agl layer

Attribute number	Meaning of the attribute
V47	Bulk Richardson Number (BRN) calculated according to Equations 3.4.57 and 3.4.58 of Bluestein (Vol. II). The surface CAPE is used in the calculation. Also, because of the volatility of BRN, I take log base 10 of the BRN for display purposes.
V48	BRN shear (kts <sup>2</sup> ). See Eq. 3.4.58 of Bluestein Vol. II.
V49	Bulk Richardson Number (BRN), except for the most unstable parcel.
V50	Temperature difference (C) between 700 and 500 mb.
V51	Magnitude (kts) of the low-level shear vector (surface to 3 km agl)
V52	Average wind speed in the 500–300 mb layer (knots)
V53	Maximum theta-e (Kelvin) in the lowest 300 mb
V54	Mean lapse rate in the 850–500 mb layer (C/km)
V55	Mean shear through a specified depth (hodograph length over a specified depth divided by that depth; *1000 s <sup>-1</sup> )
V56	Deep-layer shear vector magnitude (knots). The upper vector is the 9–11 km mean wind vector and the lower vector is the 0–2 km mean wind vector.
V57	Average parcel LCL (m agl). See NOTE above.
V58	Average RH (percent) below the surface parcel's LCL
V59	Average RH (percent) below the average parcel's LCL
V60	Vorticity Generation Potential (VGP) using the surface-based CAPE
V61	Average Mixing Ratio in 0–1 km layer (g/kg)
V62	Average Mixing Ratio in 0–3 km layer (g/kg)
V63	Average Mixing Ratio in 0–6 km layer (g/kg)
V64	Estimated 0–1 km storm relative helicity (m <sup>2</sup> /s <sup>2</sup> )
V65	Estimated 0–2 km storm relative helicity (m <sup>2</sup> /s <sup>2</sup> )
V66	Average Relative Humidity in 0–1 km layer (%)
V67	0–1 km shear magnitude (knots)
V68	0–3 km shear magnitude (knots)
V69	27% most-unstable parcel EL (corresp. to 0–3 km) shear magnitude (knots)
V70	55% most-unstable parcel EL (corresp. to 0–6 km) shear magnitude (knots)
V71	0–18% most-unstable parcel EL (corresp. to 0–2 km) storm-relative flow (knots)

Attribute number	Meaning of the attribute
V72	36–55% most-unstable parcel EL (corresp. to 4–6 km) storm–relative flow (knots)
V73	82–100% most-unstable parcel EL (corresp. to 9–11 km) storm–relative flow (knots)
V74	Level of Maximum Buoyancy from most-unstable parcel (m AGL)
V75	Maximum Buoyancy (from most-unstable parcel) (m <sup>2</sup> /s <sup>2</sup> )
V76	Level of Maximum Buoyancy from most-unstable parcel (corresp. to 0–6 km) shear magnitude (knots)
V77	20% below Level of Maximum Buoyancy from most-unstable parcel (corresp. to 4–6 km) storm–relative flow (knots)
V78	Low–Level (Most–unstable–parcel LFC to Most-unstable-parcel LFC+1km) Lapse Rate (C/km)
V79	Normalized most–unstable parcel CAPE [divide by z (Most-unstable parcel EL) – z (Most-unstable parcel LFC)]
V80	Most-unstable parcel CAPE Most–unstable parcel CAPE from Most-unstable parcel LFC to Most-unstable parcel LFC+3km
V81	Most–unstable parcel CAPE from Most-unstable parcel LFC to Most-unstable parcel LFC+3km divided by Most-unstable parcel CAPE (% age of total)
V82	Most-unstable parcel CAPE from surface to 3 km AGL
V83	Most-unstable parcel CAPE from surface to 3 km AGL divided by Most-unstable parcel CAPE (% age of total)

## References

- Adlerman E.J., Droegemeier K.K., Davies-Jones R. (1999) A numerical simulation of cyclic mesocyclogenesis. *Journal Atmospheric Science* (56), 2045–2069.
- Adrianto I., Trafalis T.B., Lakshmanan V. (2009) Support vector machines for spatiotemporal tornado prediction. *International Journal of General Systems* (38(7)), 759–776.
- Aizerman M., Aleskerov F. (1995) *Theory of Choice*. Elsevier, North-Holland.
- Aleskerov F., Cinar Y. (2008) “q-Pareto-scalar” Two-stage Extremization Model and its Reducibility to One-stage Model, *Theory and Decision* (65), 291–304.
- Aleskerov F., Mitichkin E., Chistyakov V., Shvydun S., Iakuba V. (2014) Method for selecting valid variants in search and recommendation systems (variants), *World Intellectual Property Organization, Patent Scope, Certificate, Publication Number WO/2014/148948, International Application Number PCT/RU2013/001180, Publication Date 25.09.2014, International Filing Date 27.12.2013*
- Breiman L. (2001) Random Forest. *Machine Learning* (45(1)), 5–32.
- Kingfield D.M., LaDue J.G., Ortega K.L. (2012) An evaluation of tornado intensity using velocity and strength attributes from the WSR-88D mesocyclone detection algorithm. *Preprints, 26th Conf. on Severe Local Storms, Amer. Meteor. Soc.*, 3.2.
- Lakshmanan V., Stumpf G., Witt A. (2005) A neural network for detecting and diagnosing tornadic circulations using the mesocyclone detection and near storm environment algorithms. *21st International Conference on Information Processing Systems, San Diego, CA, Amer. Meteor. Soc.*, CD-ROM J5.2.
- Lee B.D., Wilhelmson R.B. (1996) The Numerical Simulation of Non-Supercell Tornadogenesis. Part I: Initiation and Evolution of Pretornadic Mesocyclone Circulations along a Dry Outflow Boundary. *Journal of the Atmospheric Sciences* (54), 32–60.
- Markowski P.M., Richardson Y.P. (2009) Tornadogenesis: Our current understanding, forecasting considerations, and questions to guide future research. *Atmospheric Research* (93), 3–10.
- Marzban C. (2000) A neural network for tornado diagnosis. *Neural Computing and Applications* (9), 133–141.
- Marzban C., Stumpf G. (1996) A neural network for tornado prediction. *J. App. Meteo.* (35), 617.

- Natarajan D. (2011) Numerical Simulation of Tornado-like Vortices. *Electronic Thesis and Dissertation Repository* (89).
- Rasmussen E.N., Straka J.M., Davies-Jones R., Doswell C.A., Carr F.H., Eilts M.D., MacGorman D.R. (1994) Verification of the Origins of Rotation in Tornadoes Experiment: VORTEX. *Bulletin of the American Meteorological Society* 75(6), 995–1006. doi:10.1175/1520-0477(1994)075<0995:votoor>2.0.co;2/
- Richman M.B., Trafalis T.B., Adrianto I. (2008) Missing data imputation through machine learning algorithms. *Chapter 4, Artificial Intelligence Methods in the Environmental Sciences*, Haupt, et al., Eds., Springer, 153–169.
- Rhodes C.L., Senkbeil J.C. (2014) Factors contributing to tornadogenesis in land-falling Gulf of Mexico tropical cyclones, *Meteorological Applications*, 21, 940–947.
- Roberts R.D., Wilson J.W. (1995) The genesis of three nonsupercell tornadoes observed with dual-Doppler radar. *Mon. Weather* (123), 3408–3436.
- Rodriguez J.J., Kuncheva L.I., Alonso C.J. (2006) Rotation forest: a new classifier ensemble method. *IEEE Trans Pattern Anal Mach Intell* (28(10)), 1619–1630.
- Roebber P.J. (2009) Visualizing multiple measures of forecast quality. *Weather Forecast* (24), 601–608.
- Shvydun S. (2015) NORMATIVE PROPERTIES OF MULTI-CRITERIA CHOICE PROCEDURES AND THEIR SUPERPOSITIONS: I (Preprint), Series WP7 “Mathematical methods for decision making in economics, business and politics”.
- Shvydun S. (2015) NORMATIVE PROPERTIES OF MULTI-CRITERIA CHOICE PROCEDURES AND THEIR SUPERPOSITIONS: II (Preprint), Series WP7 “Mathematical methods for decision making in economics, business and politics”.
- Straka J.M., Rasmussen E.N., Davies-Jones R.P., Markowski P.M. (2007) An observational and idealized numerical examination of low-level counterrotating vortices toward the rear flank of supercells. *E.J. Severe Storms Met.* (2(8)), 1–22.
- Trafalis T.B., Adrianto I., Richman M.B., Lakshmivarahan S. (2014) Machine-learning classifiers for imbalanced tornado data. *Computational Management Science* (11), 403–418.
- Wakimoto R.M., Wilson J.W. (1989). Non-supercell tornadoes. *Mon. Weather* (117), 1113–1140.

## **Построение эффективной модели машинного обучения для предсказания торнадо**

[Текст] : препринт WP7/2016/05 / Ф. Алескеров, Н. Байбородов, С. Демин, М. Ричман, Т. Трафалис, С. Швидун, В. Якуба ; М. : Нац. исслед. ун-т «Высшая школа экономики». – М. : Изд. дом Высшей школы экономики, 2016. – (Серия WP7 «Математические методы анализа решений в экономике, бизнесе и политике»). – 24 с. – 35 экз. (на англ. яз.)

Изучены существующие методы предсказания торнадо, а также основные механизмы возникновения этих природных катастроф. Построена модель, основанная на методе суперпозиции. Для проверки эффективности построенная модель была протестирована на реальных данных, полученных из Университета Оклахомы (США).

Предложенная модель предсказания торнадо значительно превосходит предыдущие методы с точки зрения эффективности.

*Алескеров Фуад* – Национальный исследовательский университет «Высшая школа экономики», Институт проблем управления Российской академии наук им. В.А. Трапезникова, Москва, Российская Федерация.

*Байбородов Никита* – Московский физико-технический институт, Москва, Российская Федерация.

*Демин Сергей* – Национальный исследовательский университет «Высшая школа экономики», Москва, Российская Федерация.

*Ричман Майкл* – Университет Оклахомы, США.

*Трафалис Теодор* – Университет Оклахомы, США.

*Швидун Сергей* – Национальный исследовательский университет «Высшая школа экономики», Институт проблем управления Российской академии наук им. В.А. Трапезникова, Москва, Российская Федерация.

*Якуба Вячеслав* – Национальный исследовательский университет «Высшая школа экономики», Институт проблем управления Российской академии наук им. В.А. Трапезникова, Москва, Российская Федерация.

**Препринты Национального исследовательского университета  
«Высшая школа экономики» размещаются по адресу: <http://www.hse.ru/org/hse/wp>**

*Препринт WP7/2016/05*  
*Серия WP7*  
Математические методы анализа решений  
в экономике, бизнесе и политике

Алескеров Фуад, Байбородов Никита, Демин Сергей, Ричман Майкл,  
Трафалис Теодор, Швыдун Сергей, Якуба Вячеслав

**Построение эффективной модели машинного обучения  
для предсказания торнадо**  
(на английском языке)

Зав. редакцией оперативного выпуска *А.В. Заиченко*  
Технический редактор *Ю.Н. Петрина*

Отпечатано в типографии  
Национального исследовательского университета  
«Высшая школа экономики» с представленного оригинал-макета  
Формат 60×84  $\frac{1}{16}$ , Тираж 35 экз. Уч.-изд. л. 1,3  
Усл. печ. л. 1,4. Заказ № . Изд. № 1975

Национальный исследовательский университет  
«Высшая школа экономики»  
125319, Москва, Кочновский проезд, 3  
Типография Национального исследовательского университета  
«Высшая школа экономики»